High-peak-power passively Q-switched 1.3 μm Nd:YAG/V^{3+}:YAG laser pumped by a pulsed laser diode

Zhaowei Wang (王兆伟) Baitao Zhang (张百涛)*, Jian Ning (宁 建), Xiaotong Zhang (张晓彤), Xiancui Su (苏现翠), and Ruwei Zhao (赵如薇)

State Key Laboratory of Crystal Materials, Institute of Crystal Materials, Shandong University, Ji'nan 250100, China

**Corresponding author: bai3697@126.com*

Received September 24, 2014; accepted November 14, 2014; posted online February 9, 2015

We demonstrate a high-pulse-energy, short-pulse-width passively Q-switched (PQS) Nd:YAG/V^{3+}:YAG laser at 1.3 μm, which is end-pumped by a pulsed laser diode. During the PQS regime, a maximum total output pulse energy of 3.3 mJ is obtained under an absorbed pump pulse energy of 21.9 mJ. Up to 400 μJ single-pulse energy is realized with the shortest pulse width of 6.16 ns and a pulse repetition frequency of 34.1 kHz, corresponding to a peak power of 64.9 kW. The high-energy laser pulse is operated in the dual wavelengths of 1319 and 1338 nm, which is a potential laser source for THz generation.

OCIS codes: 140.3480, 140.3538, 140.3540, 140.3580.
doi: 10.3788/COL201513.021403.

High-energy solid-state lasers are found in a wide variety of applications in the fields of optical communications, micro-manufacturing, remote sensing, medical surgery, optical parametric oscillators, Raman laser pumps, and so on. Therefore, extremely high-peak-power laser sources have attracted much attention and constitute an active research topic in the laser field[1–3]. The passively Q-switched (PQS) technique can provide such laser sources and significantly improve the compactness and portability because it does not need additional complicated controllers. Moreover, it can shorten the pulse width and enhance the peak power by using a miniature-cavity configuration.

Peak-power scaling lasers have been widely investigated at 1.0 μm[4,5], whereas few studies have been dedicated to that at 1.3 μm due to the larger quantum defect and smaller emission cross section. Generally, PQS lasers can produce pulses with dozens of nanoseconds duration and relatively low peak power at 1.3 μm[6,7]. Recently, some encourage results have been achieved in the peak power or pulse width at 1.3 μm. A high-peak-power Nd:YAG/V^{3+}:YAG PQS laser by means of a flash-lamp-pump was reported[8]. They obtained laser pulses with 115 kW peak power and 86.9 ns pulse duration at 1.32 μm[8]. However, its high-peak-power pulses were produced at the expense of very low pulse repetition frequency (PRF). Laser pulses of 1.7 ns pulse duration with a Nd:YAG/V^{3+}:YAG microchip [4 mm long Nd:YAG laser crystal and 0.7 mm long V^{3+}:YAG saturable absorber (SA)] at 1338 nm was reported[9]. However, the microchip laser was limited by thermal effects, resulting in lesser peak power (20 kW). Therefore, more efforts should be made for large laser pulses of high energy and short pulse width (synchronously) at 1.3 μm. Because the operation of pulsed diode-pumps can significantly reduce the thermal effects of the gain medium and SA, it provides a promising way to generate more energetic pulses. Consequently, a peak-power scaling laser source can be attained by the combination of the PQS technique and pulsed diode-pump operation at 1.3 μm.

In this Letter, we demonstrate diode-end-pumped Nd:YAG lasers operating at 1.3 μm in both the free-running and PQS regimes. During free-running operation, a maximum output pulse energy of 9.2 mJ was achieved under an absorbed pump pulse energy of 21.9 mJ, giving an optical-optical conversion and a slope efficiency of 42% and 47%, respectively. With V^{3+}:YAG as the SA, a maximum total output pulse energy of 3.3 mJ was obtained. Up to 400 μJ single-pulse energy was attained with the shortest pulse width of 6.16 ns and a PRF of 34.1 kHz, corresponding to a peak power of 64.9 kW. A PQS laser with high-pulse-energy and short-pulse-width was realized simultaneously at 1.3 μm.

Figure 1 shows a schematic diagram of the diode-end-pumped Nd:YAG laser experiment. A simple plane-plane cavity was designed with a length of 25 mm. A fiber-coupled 30 mJ pulse laser diode (LD) with a central wavelength of 808 nm was employed as a pump source in our

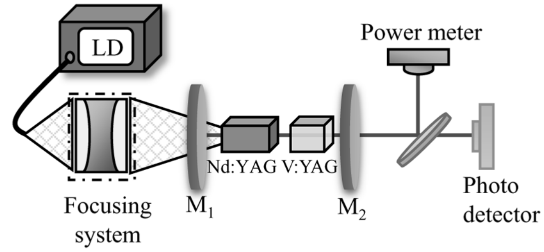

Fig. 1. Experimental configuration for the Nd:YAG/V^{3+}:YAG laser.

work. It was set to produce pump pulses of 250 μs width by adjusting the duty cycle and single period of 1.5 ms, corresponding to a repetition rate of 667 Hz. The pump beam was collimated and focused into the gain medium with a spot radius of around 300 μm through a focusing system. M_1 is a plane input mirror, which was anti-reflection (AR) coated at 808 nm on the entrance surface, high-reflection (HR, $R > 99.8\%$)-coated at 1.3 μm, and high-transmission (HT, $T > 95\%$)-coated at 808 nm on the opposite surface. The output coupler (OC) M_2 was a flat mirror with different transmissions of 15%, 25% and 30% at 1.34 μm, and HT-coated at 1064 nm to suppress the oscillation of the 1064 nm laser. The Nd:YAG crystal was 1.1 at.% Nd-doped with dimensions of 3 mm × 3 mm× 8 mm. It was covered with a thin layer indium foil and put in a water-cooled copper block in order to dissipate the heat deposition efficiently. During our work, the cooler was maintained at a temperature of 293 K. Both ends of the crystal were polished and AR-coated at a pump wavelength of 808 nm. The V^{3+}:YAG SA with dimensions of 3 mm × 3 mm × 8.6 mm and 3 mm × 3 mm × 5.8 mm was placed next to the OC to enable Q-switching operation. Its initial transmission at around 1.3 μm was measured to be 85% and 90%, respectively. The laser pulse signal was recorded with a Tektronix DPO7104 digital oscilloscope (1 GHz bandwidth, 5 Gs/s sampling rate) and a photodetector (New Focus, Model 1611). The spectrum and output pulse energy were measured with a spectrograph (0.5 nm spectral resolution, Avantes) and a laser power meter (Fieldmax-II, Coherent), respectively.

Until now, several types of SAs, such as the semiconductor saturable absorber mirror (SESAM) and Co^{2+}-doped crystals, have been successfully employed for 1.3 μm PQS lasers[10,11]. Compared with these SAs, V^{3+}:YAG crystals have many advantages, such as a relatively shorter absorption recovery time of about 5 ns, a lower saturable energy intensity of 0.05 J/cm^2, and a lower threshold. The ratio (defined as β) of its excited state absorption cross section ($\sigma_{\mathrm{esa}} = 7.4 \times 10^{-19}$ cm^2) to the ground-state absorption cross section ($\sigma_{\mathrm{gsa}} = 7.2 \times 10^{-18}$ cm^2) is about 0.1, which is useful for reducing the loss of excited-state absorption. According to the Degnan model[12], a higher ratio $\alpha = \sigma_{\mathrm{gsa}}/\sigma_{\mathrm{em}}$ was beneficial to shorten the pulse width and increase the output energy of PQS lasers for a definite pump level, where σ_{em} is the stimulated emission cross section of gain medium. With a V^{3+}:YAG crystal as the SA, the α for different Nd-doped host crystals was calculated in Ref. [6], which demonstrated the preferable candidates of Nd:YAG, Nd:KGW, and Nd:YLF gain media. Nd-doped disordered crystals have become an active field of research in recent years[13]; they have a higher ratio α due to the small stimulated emission cross section. However, considering the pulse width of the pump source (250 μs) and the comprehensive performance of the crystals, such as the thermal conductivity and optical damage threshold, the Nd:YAG crystal was the best candidate gain medium for high-energy and peak-power pulsed lasers. Therefore, the Nd:YAG gain medium and V^{3+}:YAG SA were employed for laser operation in our work.

Because of the larger quantum defect and the stronger excited-state absorption, the thermal lens effect of a Nd-doped laser at 1.3 μm was stronger than that at 1.06 μm. It is therefore desirable to minimize the thermally induced negative impact on the stability of the laser resonant cavity and laser efficiency. Consequently, the length of laser cavity was optimized to be as short as possible, which was 20 mm. Moreover, the operation pumped by a pulsed LD is also favorable for alleviating the thermal effects, which contribute to a pulse generation of short width and high energy. First, by removing the V^{3+}:YAG crystal from the cavity, the free-running regime was realized. The absorption efficiency of the Nd:YAG crystal was measured to be 89% at 808 nm. Figure 2 shows the output pulse energy attained during free-running operation for different OCs of 15%, 25%, and 30%. As shown in Fig. 2, laser thresholds of pump pulse energy increase from 2.8, 3.1, to 3.5 mJ with the augmentation of the OC transmission. The laser output pulse energy increased almost linearly in accordance with the absorbed pump pulse energy. Under an absorbed pump pulse energy of 21.9 mJ, a maximum output pulse energy of 9.2, 7.7, and 5.9 mJ (respectively) was obtained. The most efficient free-running mode was realized with a 15% OC, giving an optical–optical conversion and a slope efficiency of 42% and 47%, respectively. At the same time, the spectrum was measured (Fig. 2, inset), in which the laser emission wavelengths of 1319 and 1338 nm can be seen. Such two radiations correspond to the same transition of ${}^4F_{3/2} - {}^4F_{11/2}$, which will induce competition of the inversion populations. It was obviously observed in our work. Even so, such dual-wavelength operation was independent of the pump pulse energy.

The PQS operation of the Nd:YAG laser at 1.3 μm was performed by inserting a V^{3+}:YAG crystal with an initial transmission of 85% and 90% as the SA into the cavity. Figure 3 depicts the dependence of the total output pulse

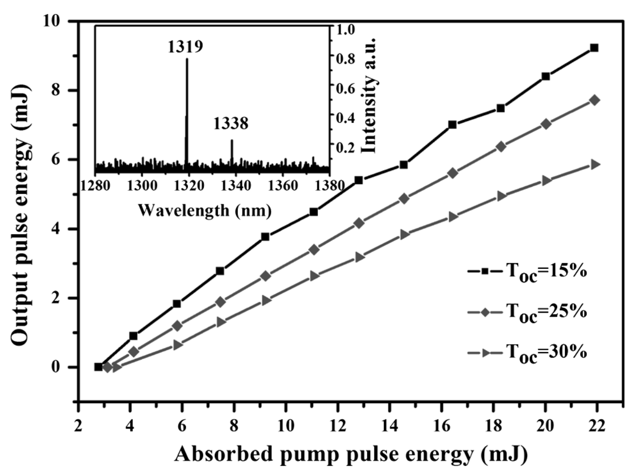

Fig. 2. Output pulse energy versus absorbed pump pulse energy in free-running operation. Inset, spectrum of Nd:YAG laser emission

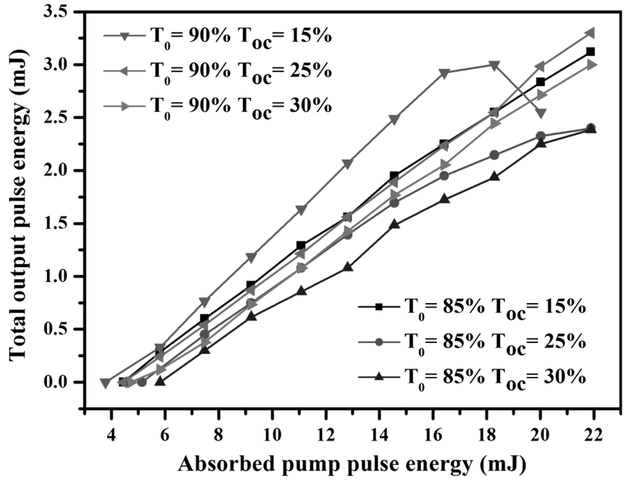

Fig. 3. PQS total output pulse energy versus absorbed pump pulse energy.

energy on the absorbed pump pulse energy. A maximum total output pulse energy of 3.3 mJ was attained under an absorbed pump pulse energy of 21.9 mJ, corresponding to an optical-to-optical conversion efficiency and a slope efficiency of 15% and 19%, respectively. The oscillator with a SA of $T_0 = 90\%$ (initial transmission) delivered a relatively lower threshold (3.7 mJ) and higher total output pulse energy (3.3 mJ) than that of $T_0 = 85\%$, resulting from the decrease of the whole resonator loss. Nevertheless, the much higher power density resulted from the OC of low transmission gave rise to serious thermal effects and damage to the gain medium and SA. Then the resonator became unstable and the value of total output pulse energy decreased sharply, as shown in Fig. 3 (dark cyan line). The measurement on the PQS laser spectrum indicated that there is no difference with the free-running laser emission. With that dual-wavelength laser, a sum-frequency wavelength of 664 nm or a radiation source of 3.2 THz can be attained.

The variations of the PRF and pulse width in accordance with absorbed pump pulse energy are depicted in Fig. 4. It was found that the PRF increased in accordance with the enhancement of absorbed pump pulse energy, which is a typical behavior for PQS lasers. Moreover, it is noteworthy that the pulse duration slightly decreased as the absorbed pump pulse energy increased continuously, which clearly differs from the operation pumped by a continuous wave (CW) LD. Based on theoretically investigations concerning a quasi-CW pumped PQS laser, the pulse energy and duration should not depend on the pump rate. They are mainly determined by the properties of the gain medium, SA, and OC, which were confirmed in our work. Therefore, no obvious diminution of the pulse width was observed in our work. In addition, the higher PRF can be fulfilled with SA of higher initial transmission. Under an absorbed pump pulse energy of 18.3 mJ, a maximum PRF of 77.5 kHz was obtained with an OC of 15% and SA of $T_0 = 90\%$. A minimum pulse width of 6.16 ns was obtained with a 25% OC and SA of $T_0 = 85\%$ under

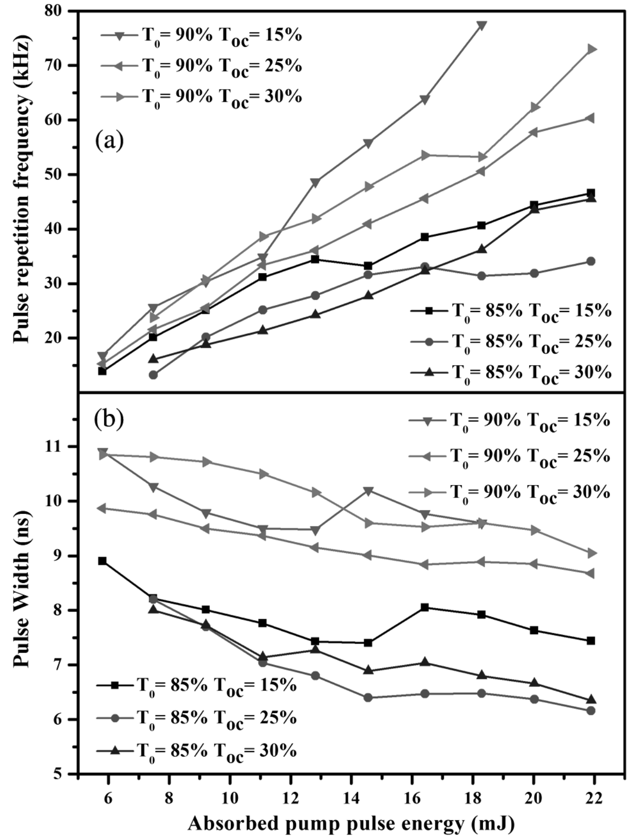

Fig. 4. (a) Variation of PRF with absorbed pump pulse energy; (b) variation of pulse width with absorbed pump pulse energy.

an absorbed pump pulse energy of 21.9 mJ, which corresponds to a total output pulse energy of 2.4 mJ and a PRF of 34.1 kHz. The temporal pulse profiles and pulse train for the previously mentioned situation are displayed in Figs. 5 and 6(b). Therefore, the single-pulse energy and peak power were calculated to be as high as 400 μJ and 64.9 kW. The results presented in this Letter prove to be a significant improvement on lasers with high pulse energy and short pulse width simultaneously. Figure 6 shows the typical Q-switched pulse train of pulsed LD and PQS lasers. When the PQS laser operated near the pump threshold, there is only one PQS laser pulse during a single pump cycle, which corresponds to Fig. 6(a). At this time, the PRF of PQS laser was the same as that of pump source (667 Hz). Further increase of the pump pulse energy would

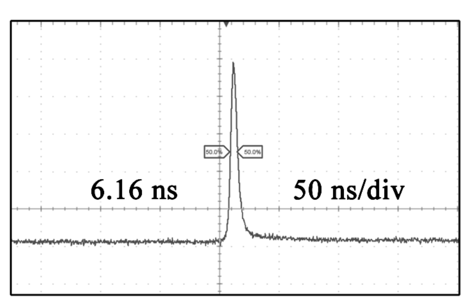

Fig. 5. Temporal pulse profile with a pulse width of 6.16 ns.

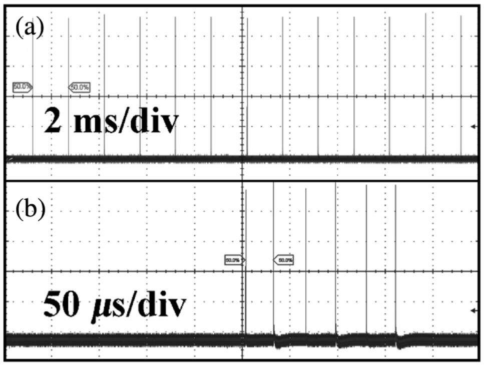

Fig. 6. Typical Q-switched pulse train. (a) Under an absorbed pump pulse energy of 5.8 mJ; (b) under an absorbed pump pulse energy of 16.4 mJ.

cause more pulses produced during a single pump pulse, illustrated in Fig. 6(b).

The basic theoretical model for PQS laser was well demonstrated in Ref. [14]. As the absorption cross section of the SA is much greater than the cross section of the lasing transition, the pulse width is described by

$$t_w = \frac{S_p t_{\mathrm{rt}}}{\gamma_{\mathrm{sat}}}\left[\frac{\delta(1+\delta)\eta}{\delta - \ln(1+\delta)}\right], \quad (1)$$

where $t_{\mathrm{rt}}(t_{\mathrm{rt}} = 2l/c)$ is the round-trip transit time of light within the laser cavity l, δ is the ratio of saturable to unsaturable cavity losses, η is the energy extraction efficiency of the laser pulse, S_p is the pulse-shape factor (typically 0.86 for Q-switched laser pulses), $\gamma_{\mathrm{sat}} = -\ln(1-\Gamma_{\mathrm{sat}})$ is the round-trip saturable loss constant, with the round-trip saturable loss of Γ_{sat}. The pulse width nearly approaches its minimum value of $t_{\mathrm{wm}} = (4S_p t_{\mathrm{rt}})/(\gamma_{\mathrm{sat}})$ under the condition of large unsaturated losses

$$\gamma_{\mathrm{par}} + \gamma_{\mathrm{op}} \gg \gamma_{\mathrm{sat}}, \quad (2)$$

where $\gamma_{\mathrm{par}} = -\ln(1-\Gamma_{\mathrm{par}})$ is the round-trip unsaturated intracavity parasitic loss constant, with the round-trip unsaturable intracavity parasitic loss of Γ_{par}, $\gamma_{\mathrm{op}} = -\ln(1-\Gamma_{\mathrm{op}})$ being the output coupling loss constant, with transmission through the OC of Γ_{op}. Owing to the high OC transmittance of 25% and low round-trip saturable loss ($\Gamma_{\mathrm{sat}} = 0.078$), Eq. (2) was obviously amenable in the limitation of our work. Based on the previously mentioned theoretical model, the pulse duration t_{wm} was calculated to be 5.62 ns with a SA of $T_0 = 85\%$ and 25% OC. The calculated result shows a roughly agreement with the experimental results (6.16 ns). Such discrepancy between them is a consequence of the heat damage and thermal lens effect on the gain medium and SA, which will broaden the duration of the laser pulse. Additionally, the theoretical model ignored spatial variations of the intracavity photon density, the population-inversion density of the gain medium, and the ground-state population density of the SA, which will introduce inaccuracy to the calculation of pulse duration.

In conclusion, we achieve both the free-running and PQS regimes for a Nd:YAG laser at 1319 and 1338 nm, end-pumped by a pulsed LD. A maximum free-running output pulse energy of 9.2 mJ is achieved under an absorbed pump pulse energy of 21.9 mJ, giving an optical-optical conversion efficiency and a slope efficiency of 42% and 47%, respectively. With V^{3+}:YAG as the SA, a maximum total output pulse energy of 3.3 mJ is obtained. Up to 400 μJ single pulse energy is realized with the shortest pulse width of 6.16 ns and a PRF of 34.1 kHz, corresponding to the peak power of 64.9 kW. The results presented in this Letter prove to be a significant improvement on lasers with simultaneous high-pulse-energy and short-pulse-width. The dual-wavelength operation with large-pulse-energy and short-pulse-width should be useful for THz generation.

This work was supported by the National Natural Science Foundation of China (Grant Nos. 61275142 12751426, 1308042, 31608042, and 51321091), the China Postdoctoral Science Foundation (Grant No. 2014T70633), and the Foundation for Outstanding Young Scientists in Shandong Province (Grant No. BS2012ZZ001).

References

1. Y. P. Huang, Y. J. Huang, and C. Y. Cho, Laser Phys. Lett. **11**, 095001 (2014).
2. D. Barry Coyle, P. R. Stysley, D. Poulios, R. M. Fredrickson, R. B. Kay, and K. C. Cory, Opt. Laser Technol. **63**, 13 (2014).
3. L. Zhang, Z. Zhuo, R. Wei, Y. Wang, X. Chen, and X. Xu, Chin. Opt. Lett. **12**, 021405 (2014).
4. H. Sakai, H. Kan, and T. Taira, Opt. Express **16**, 19891 (2008).
5. M. Gao, F. Yue, T. Feng, J. Li, and C. Gao, Chin. Opt. Lett. **12**, 021404 (2014).
6. J. K. Jabczynski, K. Kopczynski, Z. Mierczyk, A. Agnesi, A. Guandalini, and G. C. Reali, Opt. Eng. **40**, 2802 (2001).
7. A. V. Podlipensky, K. V. Yumashev, N. V. Kuleshov, H. M. Kretschmann, and G. Huber, Appl. Phys. B **76**, 245 (2003).
8. J. Ma, Y. Li, Y. Sun, and X. Hou, Laser Phys. **18**, 393 (2008).
9. J. Sulc, H. Jelinkova, K. Nejezchleb, and V. Skoda, Solid State Lasers Ampl. II **6190**, B1900 (2006).
10. H. T. Huang, J. L. He, C. H. Zuo, H. J. Zhang, J. Y. Wang, Y. Liu, and H. T. Wang, Appl. Phys. B **89**, 319 (2007).
11. R. Fluck, B. Braun, E. Gini, H. Melchior, and U. Keller, Opt. Lett. **22**, 991 (1997).
12. J. J. Degnan, IEEE J. Quantum Electron. **31**, 1890 (1995).
13. Z. W. Wang, X. W. Fu, J. L. He, Z. T. Jia, B. T. Zhang, H. Yang, R. H. Wang, X. M. Liu, and X. T. Tao, Laser Phys. Lett. **10** 055005 (2013).
14. J. J. Zayhowski and C. Dill, Opt. Lett. **19**, 1427 (1994).